Catalysis Communications 65 (2015) 24–29

Contents lists available at ScienceDirect

Catalysis Communications

journal homepage: www.elsevier.com/locate/catcom

Short communication

Fabrication of Ta_2O_5 films on tantalum substrate for efficient photocatalysis

Juxia Li, Weili Dai *, Guangjun Wu, Naijia Guan, Landong Li *

Key Laboratory of Advanced Energy Materials Chemistry of Ministry of Education, Collaborative Innovation Center of Chemical Science and Engineering (Tianjin), Nankai University, Tianjin 300071, China

ARTICLE INFO

Article history:
Received 30 November 2014
Received in revised form 5 January 2015
Accepted 4 February 2015
Available online 17 February 2015

Keywords:
Ta_2O_5 films
Hydrothermal route
Morphology
Photocatalysis
Hydrogen production

ABSTRACT

Ta_2O_5 films have been successfully fabricated on tantalum substrate via a facile hydrothermal route and characterized by a series of spectroscopic techniques. The morphology of the as-prepared Ta_2O_5 films showed great impacts on the photocatalytic activity. Without any co-catalysts, the as-prepared Ta_2O_5 films on tantalum exhibited remarkable photocatalytic activity and recyclability both in the degradation of rhodamine B and in the hydrogen production from water splitting under UV irradiation.

1. Introduction

As a semiconductor with a wide band gap, Ta_2O_5 is an important type of photocatalyst, as an alternative of TiO_2, and has been successfully applied in the photo-degradation of dyes and hydrogen production from water splitting [1–6]. Most investigations are focused on the Ta_2O_5 photocatalyst in its powder form, which is difficult for separation after reaction and unfeasible for recyclable [2–4]. In this context, exploring Ta_2O_5-based photocatalyst films is of great practical significance. Choi [7] reported that the light absorption and carrier collection were in competition over the thin films, i.e., thick films were needed to harvest a reasonable amount of the solar spectrum, but thicker films than the carrier diffusion length would result in poor carrier collection efficiency. In contrast, tantalate nanotube array films have been developed as good photocatalysts with increased light scattering, which could increase the light absorption and enhance of conversion efficiency [8–11].

Despite of the current achievements on the strategies to promote the photocatalytic activity over tantalates, the direct application of Ta_2O_5 film as photocatalyst with adequate activity is still being explored. Inspired by the pioneer work, herein, we report the fabrication of vertically stacked Ta_2O_5 films and their applications as photocatalysts in the degradation of rhodamine B (RhB) and hydrogen production under UV irradiation. The Ta_2O_5 films were synthesized via a facile hydrothermal route using Ta metal as precursor and substrate. The hierarchical structure of Ta_2O_5 films on Ta substrate is expected to facilitate the diffusion of the photogenerated holes to the top surface of the Ta_2O_5 films and therefore promote their photocatalytic efficiency in the photocatalytic reactions.

2. Experimental

2.1. Hydrothermal synthesis of Ta_2O_5 films

In a typical synthesis, 10 mL of NH_4F aqueous solution (1.6 M) and 10 mL of $(NH_4)_2S_2O_8$ aqueous solution (0.17–0.26 M) were mixed and stirred for 0.5 h. Then, the solution was added to 0.30–0.50 g $(NH_4)_2SO_4$ or 0.15–0.30 g $CO(NH_2)_2$ under stirring in parallel experiments. The mixture was transferred into a 30 mL Teflon-lined autoclave, and a piece of Ta substrate ($10 \times 10 \times 0.25$ mm) with a purity of 99.99% was placed in the solution. Thereafter, the mixture was heated to 180–200 °C for 24–48 h. Ta_2O_5 films on Ta substrate were separated from the liquid phase, and rinsed with de-ionized water. The final products were dried at room temperature overnight and labeled as Ta2O5-x (see Table S1 for details).

2.2. Characterization of Ta_2O_5 films

The XRD patterns of samples were recorded on a Bruker D8 ADVANCE powder diffractometer using Cu-K radiation (λ = 0.1542 nm) at a scanning rate of 4°/min in the region of 2θ = 20–60°.

The morphology and chemical composition of the as-prepared samples were analyzed by field emission scanning electron microcopy (FE-SEM, Hitachi S-4800).

* Corresponding authors.
E-mail addresses: weilidai@nankai.edu.cn (W. Dai), lild@nankai.edu.cn (L. Li).

http://dx.doi.org/10.1016/j.catcom.2015.02.006
1566-7367/

The diffuse reflectance UV–vis absorption spectra of the samples were recorded on a UV–vis spectrometer (Varian Cary 300) using $BaSO_4$ as reference.

X-ray photoelectron spectra (XPS) of samples were recorded on a Kratos Axis Ultra DLD spectrometer with a monochromated Al-Ka X-ray source ($h\nu = 1486.6$ eV).

Photoluminescence (PL) spectra of samples were recorded on a Spex FL201 fluorescence spectrophotometer.

2.3. Photocatalytic evaluation

The photocatalytic degradation of RhB was performed in a double-walled quartz cell cooled by water with a 250 W high-pressure Hg lamp (315–420 nm, main wavelength at 365 nm) as a light source. In each run, the as-prepared Ta_2O_5 film of ca. 100 mg was put into 200 mL of RhB solution (0.01 g/L) in the quartz cell. Prior to photocatalytic reaction the solution was magnetically stirred in the dark for 30 min to establish the adsorption-desorption equilibrium. The pH value of the solution was measured to be 7.5 ± 0.2. After the start of photocatalytic reaction, samples were taken at regular time intervals and analyzed by UV–vis spectrometer (Varian Cary 300).

Photocatalytic reforming of methanol (also-known as photo-catalytic water splitting with methanol as sacrificial agent) was performed in a top-irradiation-type Pyrex reaction cell connected to a closed gas circulation and evacuation system under the irradiation of Xe lamp with filter (wavelength: 320–400 nm). In a typical experiment, a catalyst sample of ca. 100 mg was put in 100 mL 10% methanol aqueous solution in the reaction cell. After evacuated for 30 min, the reactor cell was irradiated by the Xe lamp at 200 W under stirring. The evolved gas product, e.g. hydrogen, was analyzed by an on-line gas chromatograph (Varian CP-3800) equipped with thermal conductivity detector.

3. Results and discussion

3.1. Physico-chemical properties of Ta_2O_5 films

XRD patterns of products formed under different hydrothermal conditions are shown in Fig. 1a. Phase-pure Ta_2O_5 (JCPDF 25-0922) was obtained after the hydrothermal treatment of Ta substrate etching with NH_4F and $(NH_4)_2S_2SO_4$ solution under $(NH_4)_2SO_4$ or $CO(NH_2)_2$ as guiding agents. Typically, two strong diffraction peaks at 22.9° and 46.6° corresponded to the (001) and (002) facets of orthorhombic Ta_2O_5, respectively [12,13], could be identified for Ta_2O_5 films.

The optical properties of Ta_2O_5 films were studied by diffuse reflectance UV–vis spectroscopy. As shown in Fig. 1b, the absorption edges of Ta_2O_5 films appear in the region of 310–320 nm with neglectable

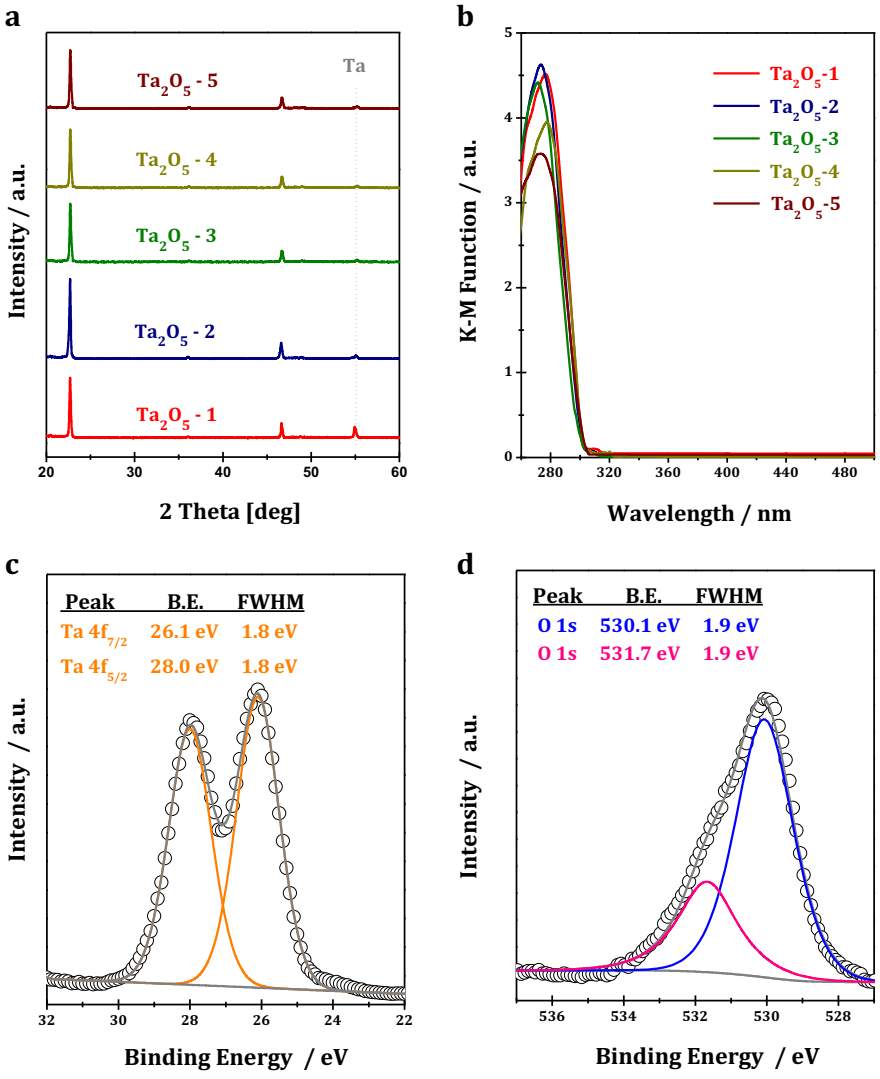

Fig. 1. (a) XRD patterns of as-prepared Ta_2O_5 films; (b) UV–vis spectra of Ta_2O_5 films; (c) Ta 4f and (d) O1s XPS of the Ta_2O_5-2. Hydrothermal synthesis conditions: temperature = 200 °C, time = 48 h.

red or blue shifts, similar to conventional Ta_2O_5. The corresponding band gaps of the Ta_2O_5 samples were ~3.9 eV, as determined from absorption onsets by plots of the square root of the Kubelka–Munk function versus photon energy [14]. The as-prepared samples are typical n-type semiconductors, which should be active in photocatalytic redox reactions under UV light irradiation.

In order to determine the chemical composition of the films and analyze the chemical state of the elements, EDS and XPS were performed on Ta_2O_5-2 which exhibited excellent photocatalytic activity in the degradation of RhB and hydrogen production (vide infra). Energy-dispersive X-ray spectroscopy (EDS) shown in Fig. S1 indicates that Ta_2O_5-2 sample is composed of Ta, O, N and F. The typical F1s peak at 684.0 eV and N1s peak at 401.6 eV in XPS are ascribed to F^- and NH_3/NH_4^+ adsorbed on the surface of Ta_2O_5, respectively, rather than the incorporation and substitution of O atoms in the orthorhombic Ta_2O_5 crystal lattice (doping) [12,15]. Fig. 1c & d shows the typical XPS of Ta4f and O1s core level. Ta 4f7/2 and Ta 4f5/2 peaks appear at 25.77 and 27.57 eV, respectively, indicating the existence of Ta species in the form of Ta^{5+} [10,16]. The O1s XPS spectrum of Ta_2O_5-2 can be fitted into two components. The major peak of lower binding energy (530.1 eV) is ascribed to the lattice oxygen (Ta–O bond) in Ta_2O_5 films while the minor peak located at 531.7 eV is ascribed to the hydroxyl group or absorbed oxygen in the surface [17]. The comparison of the possible hydroxyl groups (531. 7 eV) in the as-prepared Ta_2O_5 films, considered as an important factor influencing the photocatalytic activity, were given in Fig. S2. Nearly no changes in the O1s XPS spectrum and similar intensities of the peak at 531.7 eV can be observed, indicating that the effects of the hydroxyl groups on the photocatalytic activity in the present study can be excluded. Integrating the characterization results from XRD, EDS and XPS, we can conclude that the Ta_2O_5 films are composed of Ta_2O_5 and F species absorbed on the surface.

The typical SEM images in Fig. 2 show the surface morphology of the Ta_2O_5 films on a Ta sheet. The top and side views of a portion of the large-area Ta_2O_5 films on a Ta substrate under different hydrothermal conditions are shown in Fig. 2. The images show the vertically stacked Ta_2O_5 nanostructures with an average height of several micrometers are uniformly distributed on the whole substrate. $(NH_4)_2SO_4$ and $CO(NH_2)_2$ used as pH mediators in the present study can create different hydrothermal conditions and control the surface morphology of the Ta_2O_5 films. According to the addition of $(NH_4)_2SO_4$ or $CO(NH_2)_2$, Ta_2O_5 rods with different morphologies could be obtained (Fig. 2a–e). Typically, vertically stacked films are observed for Ta_2O_5-2 under optimized hydrothermal conditions (Fig. 2b & c). Fig. 2f shows that the Ta_2O_5-2 films with a height of 10 μm on the Ta substrate (200 μm in height).

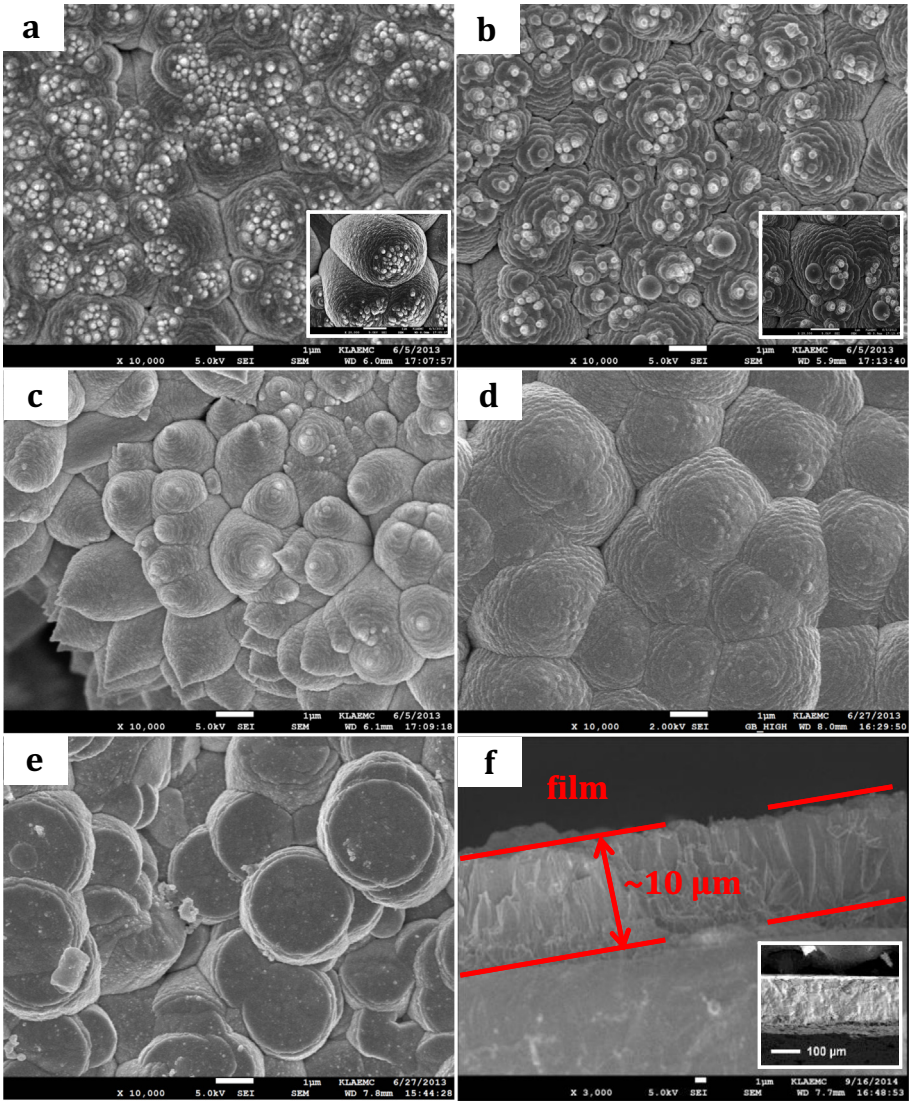

Fig. 2. SEM images of Ta_2O_5-1 (a), Ta_2O_5-2 (b), Ta_2O_5-3 (c), Ta_2O_5-4 (d), Ta_2O_5-5 (e) and cross-section of Ta_2O_5-2 (f) with and Ta substrate shown inset. Hydrothermal synthesis conditions: temperature = 200 °C, time = 48 h.

3.2. Photocatalytic performance of Ta_2O_5 films

The photocatalytic activities of the Ta_2O_5 samples (without any co-catalyst) were evaluated in the degradation of RhB and hydrogen production under UV irradiation, and the results are showed in Fig. 3. The plots of $-\ln(C/C^0)$ versus time-on-stream (TOS) catalyzed by different samples are shown in Fig. 3a. With TOS, the maximum absorption of the degraded solution appeared hypsochromic shifts, indicating the cleavage of the conjugated structure of RhB and the decomposition of a series of N-deethylated intermediates. The degradation of RhB is observed to follow pseudo-first-order kinetics. In addition, all the as-prepared Ta_2O_5 films without co-catalysts exhibit higher photocatalytic activity in RhB degradation than commercial Ta_2O_5-ref. Among the samples, Ta_2O_5-2 exhibits the highest photocatalytic activity, which is about 36 times higher than commercial Ta_2O_5-ref. The recyclability of Ta_2O_5-2 was investigated by the successive photocatalytic degradation of RhB, as shown in Fig. 3b. The photocatalyst sample was thoroughly washed with distilled water, and then directly reused for the subsequent photodegradation without thermal treatment. After five cycles, the photocatalytic performance is almost the same as that of the fresh one. It can be expected that Ta_2O_5 films show very stable photocatalytic activity, with great potential application in the treatment of dye-containing waste water.

The time course of hydrogen production from photocatalytic reforming of methanol over as-prepared Ta_2O_5 samples is shown in Fig. 3c. It is seen that all the Ta_2O_5 films exhibit considerable activity for hydrogen production from photocatalytic reforming of methanol. Similar to the results of photocatalytic RhB degradation, Ta_2O_5-2 exhibits the highest photocatalytic activity in the reforming of methanol among all the samples studied, and the highest hydrogen evolution rate of over 100 μmol h^{-1} g^{-1} could be obtained. According to the results from SEM observations (Fig. 2), the Ta_2O_5 monoliths used in the present study are dominated by the inactive Ta substrate, while Ta_2O_5 films, which are the actual photocatalysts, only possess a small part in the monoliths. According to the thickness of the Ta_2O_5 films (~10 μm) and Ta substrate (200 μm) (Fig. 2), the hydrogen evolution rate of the pure Ta_2O_5 films can be approximately calculated as 20 times of the monoliths. As a result, the highest hydrogen evolution rate of Ta_2O_5-2 can reach up to 2.3 mmol h^{-1} g_{cat}^{-1} under UV irradiation (Fig. 3d), which is really amazing [12].

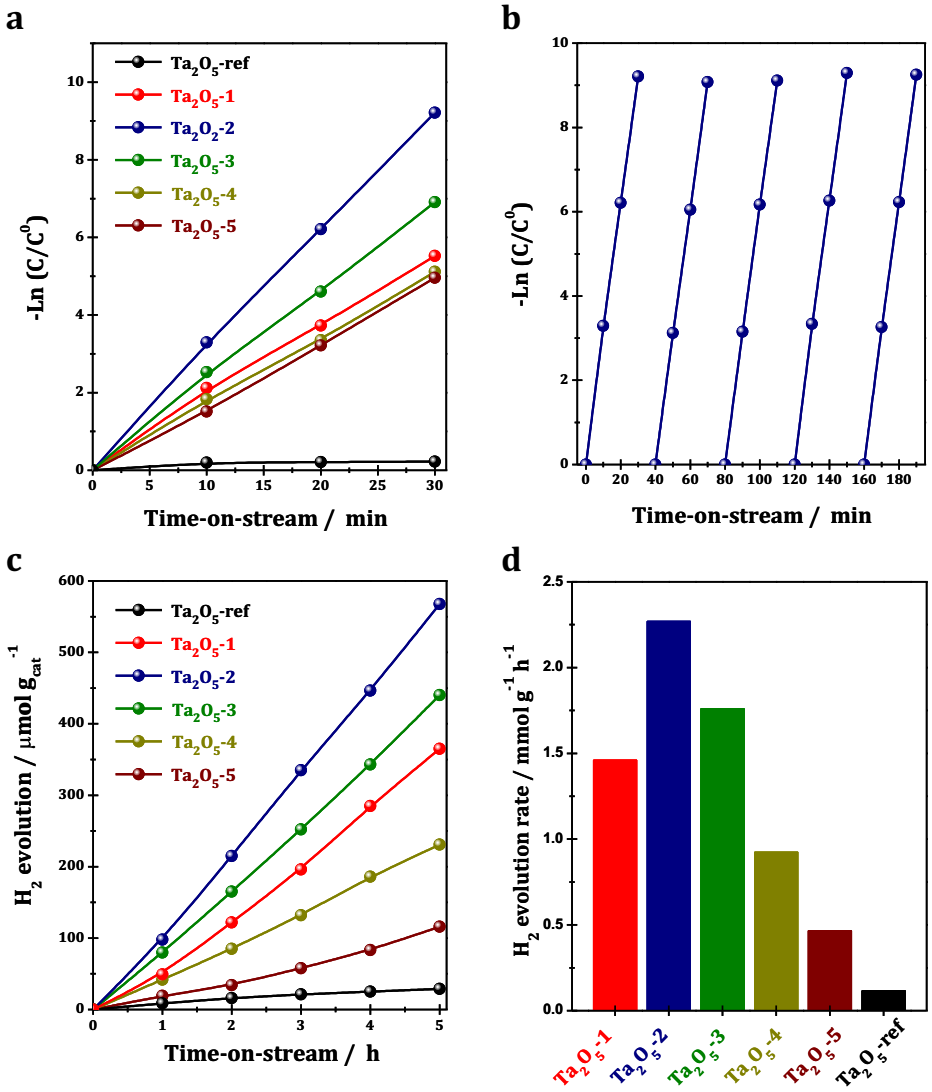

Fig. 3. (a) Photocatalytic degradation of RhB over Ta_2O_5 films and commercial Ta_2O_5-ref sample; (b) recycling of Ta_2O_5-2 in the photocatalytic degradation of RhB under UV-light irradiation; (c) photocatalytic activity of hydrogen production over the as-prepared Ta_2O_5 films and commercial Ta_2O_5 commercial Ta_2O_5-ref sample; (d) the calculated specific hydrogen production rate over Ta_2O_5 films with the subtraction of Ta substrate. Hydrothermal synthesis conditions: temperature = 200 °C, time = 48 h.

3.3. Factors controlling the photocatalytic activity of Ta_2O_5 films

The different Ta_2O_5 samples exhibited quite different photocatalytic activities. The surface area, crystal phase, morphology and crystallinity can influence the photocatalytic activity of semiconductor oxides [18]. All samples under study possess the similar surface area, similar particle size and identical orthorhombic phase with similar crystallinity. Thus, the morphology of Ta_2O_5 films is thought to be the key factor controlling the photocatalytic activity. According to Figs. 2–3 and Fig. S3–S5, the samples with some small particles on the top surfaces or with the cone-shaped top surfaces exhibited the higher photocatalytic activity than that of flat-shaped top surfaces.

An enormous enhancement on the photoelectric constant c was observed for small particles by Schmidt-Ott et al. [19], and therefore the obtained particle work function was slightly higher than the bulk and varied depending on particle sizes. Wood [20] further pointed out that this shift from bulk work function for small particles has a classical interpretation based on classical image and Coulomb potentials of spherical geometry:

$$\Phi = \Phi_\infty + \frac{e^2}{4\pi\varepsilon_0}\left(\frac{q+1}{r} - \frac{5}{8r}\right).$$

Accordingly, we propose that smaller Ta_2O_5 particles should have larger work function and the photo-generated electrons should transfer from larger particles to smaller particles under irradiation. Moreover, it is known that the semiconductor Ta_2O_5 has the higher work function than that of tantalum metal [21]. That is, the electrons should transfer from metal tantalum to semiconductor Ta_2O_5 under irradiation.

On the basis of above-mentioned issues, the separation and transfer of electron–hole pairs under irradiation are illustrated in Scheme 1. It is clearly seen that the separation of electron–hole pairs under irradiation is greatly promoted by the hierarchical structure of Ta_2O_5 films on Ta substrate and a directional flow of photo-generated electrons is revealed. As a result, the photo-generated electrons are accumulated at the top of Ta_2O_5 films, which greatly promotes their photocatalytic efficiency. Therefore, the samples possess some small particles on the top surfaces or with the cone-shaped top surfaces will exhibit higher photocatalytic activity than that of flat-shaped top surfaces.

In order to investigate the efficiency of charge carrier trapping, immigration and transfer in the Ta_2O_5 samples, room temperature emission PL spectra of Ta_2O_5 films were performed and the results are shown in Fig. 4. Two obvious signals at ca. 430 and 475 nm are observed

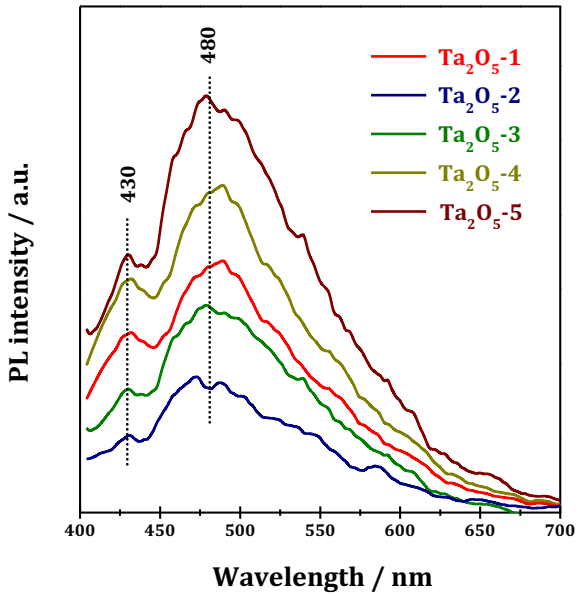

Fig. 4. Photoluminescence spectroscopy of as-prepared Ta_2O_5 films recorded at room temperature. Hydrothermal synthesis conditions: temperature = 200 °C, time = 48 h.

for all the samples, originated from the irradiative recombination of free electrons in shallow traps and sub-bands below conductive band and free holes at the valance band edge [22,23]. The changes in PL intensity correlated with the observed photocatalytic activity (i.e. lower PL intensity correlated with higher photocatalytic activity). This indicates that Ta_2O_5 films with the cone-shaped top surfaces can effectively suppress the irradiative recombination. Therefore, the Ta_2O_5-2 sample exhibited the highest activity in photocatalytic reactions.

4. Conclusion

Ta_2O_5 films have been successfully prepared via a facile hydrothermal method on Ta substrate. The morphology of the as-prepared Ta_2O_5/Ta monolith, which is controlled by the crystallization temperature and crystallization duration, shows great impacts on the photocatalytic activity. The PL results indicate that Ta_2O_5 films with the small particles on the top surface or with the tip-shaped top surfaces can effectively suppress the irradiative recombination. As a result, remarkable

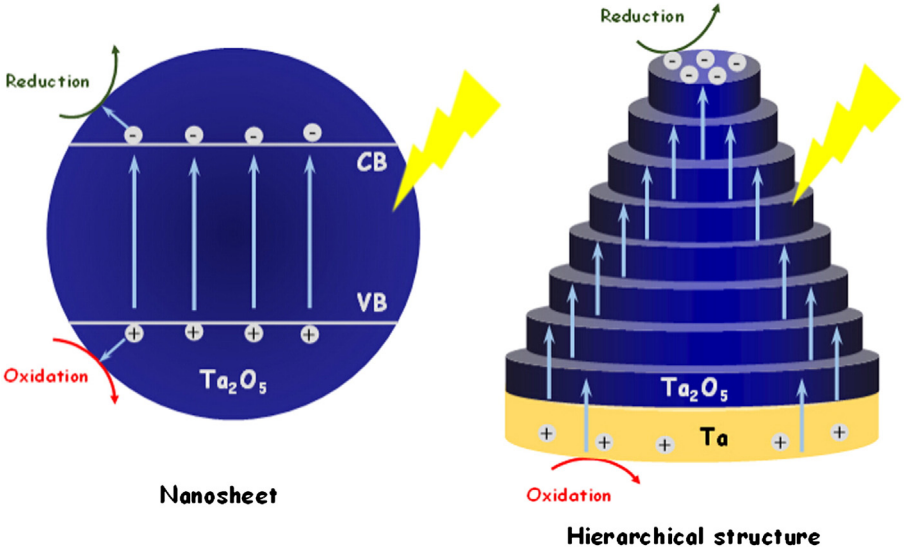

Scheme 1. Scheme of the separation and transfer of electron–hole pairs over hierarchical Ta_2O_5 films on Ta substrate under irradiation.

photocatalytic activity in the degradation of RhB and hydrogen production under ultraviolet irradiation can be obtained. Without noble-metal cocatalysts, the highest hydrogen evolution rate of Ta_2O_5 films can be up to 2.3 mmol h^{-1} g_{cat}^{-1}. It is demonstrated that Ta_2O_5 films are potential photocatalyst for application due to their simple preparation process, remarkable photocatalytic activity and good recyclability.

Acknowledgments

This work was supported by the National Natural Science Foundation of China (21421001) and the Ministry of Education of China (IRT13R30, IRT13022).

Appendix A. Supplementary data

Supplementary data to this article can be found online at http://dx.doi.org/10.1016/j.catcom.2015.02.006.

References

[1] Y. Noda, B. Lee, K. Domen, J.N. Kondo, Chem. Mater. 20 (2008) 5361–5367.
[2] J.N. Kondo, K. Domen, Chem. Mater. 20 (2008) 835–847.
[3] J. Huang, R. Ma, Y. Ebina, K. Fukuda, K. Takada, T. Sasaki, Chem. Mater. 22 (2010) 2582–2587.
[4] T. Sreethawonga, S. Ngamsinlapasathianb, S. Yoshikawa, J. Mol. Catal. A 374 (2013) 94–101.
[5] Z.X. Su, L. Wang, S. Grigorescu, K. Lee, P. Schmuki, Chem. Commun. 50 (2014) 15561–15564.
[6] T. Hisatomi, J. Kubota, K. Domen, Chem. Soc. Rev. 43 (2014) 7520–7535.
[7] K.S. Choi, J. Phys. Chem. Lett. 1 (2010) 2244–2250.
[8] S. Banerjee, S.K. Mohapatra, M. Misra, Chem. Commun. (2009) 7137–7139.
[9] X.J. Feng, T.J. LaTempa, J.I. Basham, G.K. Mor, O.K. Varghese, C.A. Grimes, Nano Lett. 10 (2010) 948–952.
[10] J. Liu, J.W. Liu, Z.H. Li, J. Solid State Chem. 198 (2013) (192–19).
[11] N.K. Allam, B.S. Shaheen, A.M. Hafez, ACS Appl. Mater. Interfaces 6 (2014) 4609–4615.
[12] J.Y. Duan, W.D. Shi, L.L. Xu, G.Y. Mou, Q.L. Xin, J.G. Guan, Chem. Commun. 48 (2012) 7301–7303.
[13] Z.H. Li, J.W. Liu, J.Y. Li, J. Shen, Nanoscale 4 (2012) 3867–3870.
[14] Z.S. Li, T. Yu, Z.G. Zou, Appl. Phys. Lett. 88 (2006) (071917-071917-3).
[15] M.H. Zhou, J.G. Yu, J. Hazard. Mater. 152 (2008) 1229–1236.
[16] E. Atanassova, G. Tyuliev, A. Paskaleva, D. Spassov, K. Kostov, Appl. Surf. Sci. 225 (2004) 86–99.
[17] Y. Lee, T. Watanabe, T. Takata, Chem. Mater. 17 (2005) 2422–2426.
[18] S. Kim, W. Choi, J. Phys. Chem. B 109 (2005) 5143.
[19] A. Schmidt-Ott, P. Schurtenberger, H.C. Siegmann, Phys. Rev. Lett. 45 (1980) 1284.
[20] D.M. Wood, Phys. Rev. Lett. 46 (1981) 749.
[21] J.L. Lan, S.J. Cherng, Y.H. Yang, Q.F. Zhang, S. Subramaniyan, F.S. Ohuchi, S.A. Jenekhe, G.Z. Cao, J. Mater. Chem. A 2 (2014) 9361.
[22] R.E. Rex, F.J. Knorr, J.L. McHale, J. Phys. Chem. C 117 (2013) 7949–7951.
[23] W. Feng, G.J. Wu, L.D. Li, N.J. Guan, Green Chem. 13 (2011) 3265–3272.